International Journal of Non-Linear Mechanics 58 (2014) 128–138

Contents lists available at ScienceDirect

International Journal of Non-Linear Mechanics

journal homepage: www.elsevier.com/locate/nlm

Pull-in instability of electrostatic doubly clamped nano actuators: Introduction of a balanced liquid layer (BLL)

E. Yazdanpanahi [1], A. Noghrehabadi *, M. Ghalambaz

Department of Mechanical Engineering, Shahid Chamran University of Ahvaz, Ahvaz, Iran

ARTICLE INFO

Article history:
Received 21 February 2013
Received in revised form
1 September 2013
Accepted 9 September 2013
Available online 17 September 2013

Keywords:
Nano actuators
Liquid layer
Pull-in instability
Modified Adomian decomposition method (MADM)

ABSTRACT

In this paper, the effect of a liquid layer, water, underneath an electrostatic nano actuator on the pull-in instability of actuator is investigated. A continuum model is employed to obtain the non-linear constitutive equation of the nano actuator and the applied forces. The governing differential equation of the actuator is forth order and highly non-linear. Hence, the modified Adomian decomposition method (MADM) is utilized to obtain an analytical solution for bucking and pull-in instability of the actuator. The results of analytical solution were compared with results of a numerical method, and they were found in good agreement. It is found that the voltage, Casimir and liquid layer parameters are the most significant parameters which affect the pull-in instability of the actuator. Interestingly, the outcomes show that there is a distinct liquid layer parameter in which the variation of the Casimir parameter does not have a significant influence on the values of maximum deflection, internal stress and bending moment of the nano actuators at the onset of pull-in instability. We introduced this value of liquid layer parameters as Balance Liquid Layer (BLL) value because of its unique effect on the maximum deflection, internal stress and bending moment of the nano actuators. The BLL value is of interest for design of NEMS actuators.

1. Introduction

Micro and Nano devices have found wide applications as sensors and actuators. The analysis of actuation and sensing methods for these devices has been a topic of interest over the past several years. The properties such as piezoresistive, piezoelectric, electrostatic, thermal, electromagnetic, and optical have been used for actuation and sensing of micro and nano switches [1].

Micro and Nano fabrication processes are planar technologies, and therefore, many micro and nano devices consist of elastic beams and plates suspended over a rigid substrate. In small scale technology, the suspended beams or plates serve as the active component of accelerometers [2], pressure sensors [3], electrical or optical switches [4], electrostatic actuators [5] and some of the digital light processing chips [6]. The nano electro mechanical switches can be constructed using nanotubes including single wall carbon nanotubes (SWCNTs) and multi wall carbon nanotubes (MWCNTs) [7].

A typical switch is constructed with two conducting electrodes, one is the substrate, which is fixed, and the other one is the suspended electrode over the substrate. Applying external force (commonly voltage or intermolecular force) would deflect the suspended electrode downward into the substrate. Theoretical and experimental studies demonstrate that there is an inherent instability, known as the pull-in instability, in both Micro Electro-Mechanical Systems (MEMS) and Nano Electro-Mechanical Systems (NEMS) switches. The pull-in instability occurs at a certain deflection (or applied voltage) when the movable electrode becomes unstable and pulls-in onto the substrate. Indeed, at the onset of pull-in instability, the elastic restoring force can no longer balance the external force. Further increasing the external force would induce a dramatic displacement jump which causes structure collapse or failure. A set of certain deflection and applied voltage, which induce the instability, is known as pull-in parameters of the switch.

Some aspects of parallel plate actuators have been studied by previous researchers. Chen et al. [8] extensively have analyzed the pull-in voltage of various geometric shapes of electrodes for parallel rigid plate actuators. Gorthi et al. [9] have studied the pull-in voltage behavior of electrostatic actuators using a beam model along with a dielectric layer. They identified three possible static configuration of the nanobeams namely, floating, pinned and flat configuration. They classified all possible transitions based on a dielectric layer parameter. Yazdanpanahi et al. [10] have

* Corresponding author. Tel.: +98 611 333 0010x5678; fax: +98 611 333 6642.
E-mail addresses: e.yazdanpnahi@gmail.com (E. Yazdanpanahi).
noghrehabadi@scu.ac.ir, a.r.noghrehabadi@scu.ac.ir (A. Noghrehabadi).
m.ghalambaz@gmail.com (M. Ghalambaz).
[1] Tel.: +98917 378 3104.

0020-7462/$ - see front matter © 2013 Elsevier Ltd. All rights reserved.
http://dx.doi.org/10.1016/j.ijnonlinmec.2013.09.001

studied the influence of capillary force on the deflection and pull-in instability of electrostatic micro actuator beams in the presence of a dielectric layer. They [10] reported a specific value of dielectric parameter in which the variation of the dimensionless capillary parameter does not affect the value of maximum deflection of the micro actuator at the onset of pull-in instability. They introduced this value of dielectric parameter as Balance Dielectric Layer (BDL) because of its unique properties. Rollier et al. [11] studied the stability conditions of parallel-plate electrostatic actuators, which are embedded in liquids. They reported that the pull-in instability can be shifted beyond one-third of the gap, and it can even be suppressed by changing the dielectric layer parameter. Abdel Rahman et al. [12], utilizing a non-linear model, have studied the effect of axial load on the instability of electrically actuated microbeams. They reported that increasing the axial force increases the pull-in electrostatic force and affects deflection of the microbeam.

The inter-molecular forces have a significant influence on the instability of the nanobeams in the nanoscale separations [13–15]. When the separation between the nanobeam and substrate is large enough (typically greater than 20 nm), retardation appears. In the presence of retardation effects, the intermolecular interaction between the two electrodes (i.e. nanobeam and substrate) can be described by the Casimir force [13,16,17]. Considering the ideal case, the Casimir force is proportional to the inverse fourth power of the separation [18,19]. The Casimir force, which is usually neglected in design of micromechanical switches, plays an important role in actuation of nanoscale switches [20,21]. Lin and Zhao [22] have studied the influence of Casimir and voltage forces on the static and dynamic behavior of nano actuators. Ramezani et al. [23,24] have utilized analytical and numerical methods to simulate pull-in instability of cantilever type nanobeam switches in the presence of intermolecular forces. The static pull-in instability of nanocantilever beams immersed in a liquid electrolyte is theoretically investigated by Noghrehabadi et al. [25]. They found that the size effect greatly influences the beam deflection and is more noticeable for small thicknesses. The findings reveal that the increase of ion concentration increases the pull-in voltage but decreases the pull-in deflection.

Recently, analytical solutions have been employed to solve non-linear governing equation of micro or nano actuators to obtain a solution for pull-in instability of these actuators [26–29]. Adomian decomposition method is an analytical method which proposed by Adomian for a wide class of dynamical systems without linearization or weak non-linearity assumptions [30]. Wazwaz [31] proposed a modification to the Adomian decomposition method in order to accelerate the rapid convergence of the series solution. The effectiveness of Modified Adomian Decomposition Method (MADM) has been demonstrated in many recent researches [32–38].

Water or water solutions are commonly used for the rinsing and drying process in the nanofabrication [39,40]. In the synthesis process or in use, a layer of water may form underneath the beam [40]. In many other applications including biological processes, wetting, corrosion [41] a layer of liquid may also form underneath of the electrode. The liquid layer acts as a dielectric and affects the pull-in parameters (i.e. pull-in voltage and pull-in deflection) of the nano actuator. To the best of the author's knowledge, the effect of presence of a liquid film on the deflection and pull-in instability of nano beam actuators has not been analyzed yet.

The objective of the present paper is to study the effect of a liquid layer on the pull-in instability of nano actuators in the presence of the Casimir force. The nano actuator is modeled as a doubly clamped beam, which is subjected to the electrical and Casimir forces. Here, in a general case, a liquid layer is considered to obtain a generalized non-dimensional form of the governing equations. However, for the calculations, a special attention is taken to the practical case of water as the liquid. The distributed parameter model of nanoswitch in its non-dimensional form depends on the non-dimensional dielectric parameter, electrical parameter, fringing field parameter and Casimir parameter. The influence of non-dimensional parameters on the pull-in instability of nanoswitches is analytically investigated.

2. Theoretical model

A nano size clamped-clamped actuator is modeled as an electrode beam with a layer of liquid underneath. Fig. 1 depicts the schematic view of the nano actuator. In this figure, H is the gap distance between the substrate and the suspended electrode. L, t and w are the length, thickness and width of the suspended electrode, respectively. The fabricated models of these nano actuator switches can be seen in the work of Hayamizu et al. [42]. The deflection of the beam, subjected to the external forces, can be evaluated using the energy method. The stored energy of the beam is the sum of elastic energy (U_b), stretching energy (U_S) and the work of external forces (W_E). The energy terms of the system are calculated as follows:

The beam bending elastic energy U_b [43,44]:

$$U_b = \frac{E'I}{2}\int_0^L \left(\frac{d^2Y}{dX^2}\right)^2 dX \tag{1}$$

where Y is the deflection of the nanobeam, X is the position along the beam measured from the one end, I is the moment of inertia of the beam with rectangular cross section (A). The effective beam

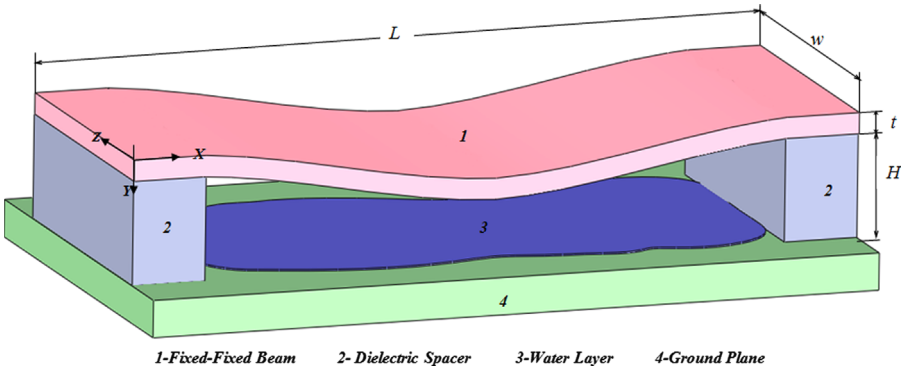

Fig. 1. Schematic representation of distributed model of fixed-fixed beam with a liquid layer.

material (E') for narrow beams ($w<5t$) becomes E and for wide beams ($w>5t$) is the plate modulus $E/(1-\nu^2)$, where ν is the Poisson ratio.

The beam stretching energy U_S is [43,45]:

$$U_s=\frac{1}{2}\frac{E'A}{2L}\left(\int_0^L\left(\frac{dY}{dX}\right)^2dX\right)^2 \tag{2}$$

where A is the cross-section area of the beam ($A=wt$).

The work done by external force f_{ex} per unit length is [43,46]

$$W_E=\int_0^L Y(x)f_{ex}dX \tag{3}$$

Thus, the total energy is written as

$$\Pi=U_b-U_s-W_E \tag{4}$$

Using the principle of virtual work (PVW: $\delta\Pi=0$), the governing equation is written as [25,43]

$$E'I\frac{d^4Y}{dX^4}-\left[\frac{E'A}{2L}\int_0^L\left(\frac{dY}{dX}\right)^2dX\right]\frac{d^2Y}{dX^2}=f_{ex}, \tag{5.a}$$

where the boundary conditions at the fixed ends are

$$Y(0)=0,\quad Y(L)=0 \tag{5.b}$$

$$Y'(0)=0,\quad Y'(L)=0 \tag{5.c}$$

The external forces, acting on the nanobeam electrode, are sum of the electrostatic force (f_{elec}) and Casimir force (f_{cas}). The electrostatic force is the result of a voltage difference (V) between the suspended electrode and the substrate. The Casimir force is the results of quantum mechanical forces and appears between beam and substrate because of the nanoscale dimension of the gape (H). As mentioned, the external forces which act on the nanobeam electrode are sum of the electrostatic force (f_{elec}) and Casimir force (f_{cas}). Therefore, the external force is written as follow:

$$f_{ex}=f_{elec}+f_{cas} \tag{6}$$

The Maxwell's equations are general and hold for fields with arbitrary time dependence in any medium and at any location. They can be reduced to the simpler forms for special cases such as static case, sinusoidal time varying (or time-harmonic) fields. In the static limit, electric and magnetic fields are independent of each other [47]. When a voltage is applied between the plate and substrate, electric charges are stored as a capacitor-like device and generate an electrostatic force. Normally, the electrostatic force is defined by Coulomb famous inverse square law. Here, the parallel-plate electrostatic actuators with the liquid layer assumed to be a series of capacitors. Considering the first order fringing field correction, the electrostatic force is written as [10,48],

$$f_{elec}=\frac{\varepsilon_0 wV^2}{2}\left[\frac{t_f}{\varepsilon_f}+H-t_f-Y\right]^{-2}+\frac{\varepsilon_0V^2}{2}\frac{0.65}{[H-Y]}, \tag{7}$$

where $\varepsilon_0=8.854\times10^{-12}$ c^2/Nm^2 is the permittivity of vacuum and ε_f and t_f are the relative permittivity and thickness of the liquid layer, respectively.

Decreasing the size of structures and materials to the scale of nanometers, a regime, in which the forces are quantum mechanical in nature, Casimir forces, appears. Indeed, for the gap, between the substrate and the beam, in the range of 100 nm or lower the Casimir force is very strong. In this case, the Casimir force is comparable with the electrostatic force, corresponding to the voltage within the range of 0.1–1.0 V [49]. For arbitrary materials, Casimir's results were generalized by Lifshitz [49]. Casimir force per unit length of the actuator between two ideal conductors is proportional to the inverse fourth power of the separation (i.e. $H-Y$). Therefore, the Casimir force between two parallel plates of the electrode and substrate is evaluated as [21,50,51]

$$f_{cas}=\frac{\pi^2\hbar\, c\, w}{240(H-Y)^4}, \tag{8}$$

where $\hbar=1.055\times10^{-34}$ Js is the reduced Planck's constant and $c=2.998\times10^8$ m/s is the light speed. When the width of the actuators is sufficiently higher than the separation gap, Eq. (8) provides acceptable results [20]. Hence, in this study, the nano actuators that are wider than the separation ($H<w$) are merely considered.

Eq. (7) Shows that the electrostatic force not only is a function of the structure and the dimensions of the nanobeam but also the applied voltage. As the electrostatic force is a function of the external applied voltage, the voltage can be adjusted regarding to the size of the beam. However, based on Eq. (8), the Casimir force is a function of the nanobeam dimensions. For a nanobeam with the width of 200 nm, separation of 20 nm, and a common voltage difference of 1 V, the Casmir force is 1.6×10^{-3} N/m and the electrostatic force is 2.3×10^{-3} N/m. The comparison between the evaluated values of Casimir force and electrostatic force show that these forces are of comparable magnitude.

Substituting Eqs. (7) and (8) into Eq. (6), and introducing the non-dimensional variables as

$$\eta=6(\frac{H}{t})^2,\ K=\frac{t_f}{\varepsilon_f H},\ \beta=\frac{\varepsilon_0 wL^4V^2}{2H^3E_{eff}I},$$
$$\gamma_{fr}=0.65\beta\frac{H}{w},\ \alpha=\frac{\pi^2\hbar\, c\, wL^4}{240\, EIH^5},\ T^*=\eta\int_0^1\left(\frac{dg}{dx}\right)^2dx \tag{9}$$

leads to the non-dimensional form of Eq. (5.a)as follow:

$$\frac{d^4g}{dx^4}-T^*\frac{d^2g}{dx^2}=-\frac{\alpha}{g(x)^4}-\frac{\beta}{(K(1-\varepsilon_f)+g(x))^2}-\frac{\gamma_{fr}}{g(x)} \tag{10.a}$$

The non-dimensional boundary conditions in non-dimensional form are

$$g(0)=1,\quad g'(0)=0, \tag{10.b}$$

$$g(1)=1,\quad g'(1)=0, \tag{10.c}$$

where $g=1-Y/H$ and prime denotes differentiation with respect to x which $x=X/L$. The non-dimensional parameters α, β, γ_{fr} and K are Casimir, applied voltage, fringing field and liquid layer parameters, respectively. Eq. (10-a) is the governing equation of nanobeam. This equation is forth order and highly non-linear. In the following section, the modified Adomian decomposition method is employed to obtain an analytical solution for this equation.

3. Mathematical solution method

The Adomian decomposition method is an analytical method for a wide class of non-linear equations which established by Adomian in 1988 [30]. Modified Adomian decomposition method proposed by Wazwaz to accelerate and rapid convergence of the Adomian series [31]. Here, the modified Adomian decomposition method [31] has been utilized to solve the governing equation of the nanobeam, Eq. (10.a), subject to the boundary equations, Eqs. (10.b) and (10.c). In order to solve Eq. (10), the recursive equation of the solution, based on the MADM, is obtained as follow (see Appendix A):

$$g(x)=d_0+d_1x+\frac{d_2x^2}{2}+\frac{d_3x^3}{6}+T^*L^{(-2)}(g(x))$$
$$-L^{(-4)}\left(\frac{\alpha}{g(x)^4}+\frac{\beta}{(K(1-\varepsilon_f)+g(x))^2}+\frac{\gamma_{fr}}{g(x)}\right), \tag{11}$$

The non-linear functions, i.e. $g(x)$, in Eq. (11) are replaced by the Adomian polynomials to obtain the recursive solution (see Appendix A) as

$$g(x)=d_0+d_1x+\frac{1}{2}d_2x^2+\frac{1}{6}d_3x^3+T^*\times L^{-(2)}\left(\sum_{n=0}^{\infty}g_n\right)-L^{-(4)}\left(\sum_{n=0}^{\infty}(\alpha\times A_n+\beta\times B_n+\gamma_{fr}\times C_n)\right) \tag{12}$$

where A_n, B_n and C_n are the Adomian polynomials of $1/g(x)^4$, $1/(K'+g(x))^2$ and $1/g(x)$, respectively (see Appendix B.1), and K' is $K(1-\varepsilon_f)$. Substituting boundary conditions at $x=0$ into Eq. (12) yields:

$$d_0=1,\quad d_1=0, \tag{13}$$

Finally, the polynomial solution of Eq. (18) is obtained by sum of three terms of Adomian polynomials, i.e. g_0, g_1 and g_2, as (see Appendix B.2):

$$\begin{aligned}g(x)=1&+\frac{1}{2}d_2x^2+\frac{1}{6}d_3x^3+T^*\frac{x^2}{2}-\left(\alpha+\frac{\beta}{(1+K')^2}+\gamma_{fr}+T^*d_2+T^{*2}\right)\frac{x^4}{24}\\&+\frac{T^*d_3}{120}x^5+\left(\frac{\alpha d_2}{180}+\frac{\alpha T^*}{240}+\frac{\beta d_2}{360(1+K')^3}+\frac{\gamma_{fr}d_2}{720}\right.\\&\left.-\frac{T^*\beta}{720(1+K')^2}+\frac{T^*\beta}{360(1+K')^3}\right)x^6\\&+\left(\frac{\alpha d_3}{1260}+\frac{\beta d_3}{2520(1+K')^3}+\frac{\gamma_{fr}d_3}{5040}\right)x^7\\&-\left(\frac{\gamma_{fr}\alpha}{8064}-\frac{\gamma_{fr}\beta}{20160(1+K')^3}-\frac{\gamma_{fr}\beta}{40320(1+K')^2}\right.\\&-\frac{\beta\alpha}{20160(1+K')^3}-\frac{\beta\alpha}{10080(1+K')^2}\\&\left.-\frac{\alpha^2}{10080}-\frac{\beta^2}{20160(1+K')^5}-\frac{\gamma_{fr}{}^2}{40320}\right)x^8,\end{aligned} \tag{14}$$

Here, the solution is depicted for three terms of the Adomian polynomials. The undetermined constants, d_2, d_3 and T^* can be evaluated by the solution of the algebraic equations which come from the boundary conditions, Eq. (10-c) at $x=1$, and the definition of T^* as follow:

$$\begin{cases}g(1)=1\\g'(1)=0\\T^*=\eta\int_0^1\left(\frac{dg}{dx}\right)^2dx\end{cases} \tag{15}$$

The number of required series terms is indicated by verifying the accuracy and convergence of the solution. To aim this purpose, the deflection of a typical nano actuator is evaluated numerically. The numerical results are compared with the results of MADM, obtained using different terms of series. The numerical results are obtained using the combination of Runge–Kutta and Gauss–Newton iteration method [52]. A maximum relative error of 10^{-10} is used as the stopping criteria. The deflection error over the non-dimensional length of the nanobeam for different terms of the MADM series is shown in Fig. 2 when $\beta=5$, $K=0.005$ and $\alpha=20$. The Error in this figure is computed using the relative error as follow:

$$Error\% = |u_{MAD}-u_{Num}|/u_{Num}\times 100, \tag{16}$$

where u denotes the ratio of beam deflection to the gap ($u=Y/H$). Here, $u_{MAD}$and u_{Num} are the mid plan deflection evaluated using MADM and numerical method, respectively. As seen in Fig. 2, the maximum error for deflection of nanobeam occurs at the middle of the beam where $x=0.5$. The corresponding maximum error deflection of the nanobeam, depicted in the Fig. 2, is brought in Table 1. The results of Table 1 show that the higher precision can be achieved by selecting more terms of the modified Adomian series. As seen, the analytical solution converges to the numerical solution by increasing the number of the selected terms of the series. The results of Fig .2 evidence that the relative error for eight terms of the modified Adomian series is less than 0.05%. Hence, eight terms of modified Adomian series are used for calculations in the following text for convenience. Fig. 3 shows the error between numerical and analytical (eight terms of Adomian series) results of

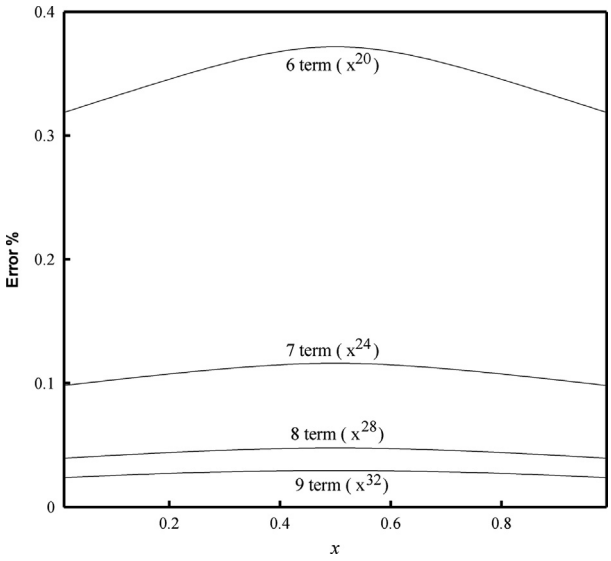

Fig. 2. The variation of the relative error due to deflection of a nanobeam and evaluated with selected terms of MADM for $K=0.005$, $\alpha=20$ and for $\beta=5$.

Table 1
The variation of the maximum deflection of a nano beam (u_{max}) evaluated with selected terms of MADM for $K=0.005$, $\alpha_4=20$ and for $\beta=5$.

Tip deflection	5 Terms (x^{16})	6 Terms (x^{20})	7 Terms (x^{24})	8 Terms (x^{28})	9 Terms (x^{32})
MADM	0.133601	0.134856	0.135202	0.135295	0.135319
Numerical			0.135359		
Error%	1.3	0.372	0.116	0.047	0.029

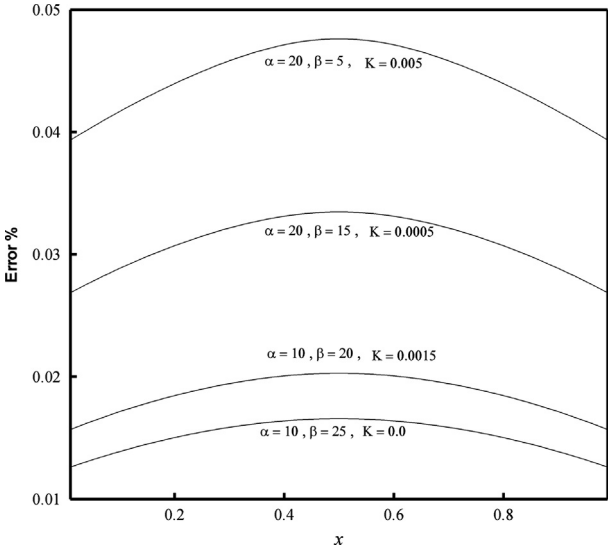

Fig. 3. The comparison of a nanobeam relative error according to difference values of K, α and β.

Table 2
A comparison between the pull-in voltages of typical microbeams evaluated using eight terms of MADM, the numerical method and the pull-in voltages reported in the previous studies.

Beam length (μm)	Pull-in voltage (V_{PI})				
	ADM [36]	(2-D model) [53]	MEMCAD [53]	Numerical (present)	MADM (present)
250	39.6	39.5	40.1	39.1	39.3
350	20.2	20.2	20.3	20.0	20.1

the beam deflection for different combinations of non-dimensional parameters. As seen, the error is very low (less than 0.05%), and the maximum error occurs at the middle of the beam where $x=0.5$.

By neglecting the Casimir and stretching effects ($\alpha=0$, $\eta=0$) and in the absence of liquid layer, the present study reduces to the study of the pull-in instability of a microbeam. Therefore, in this case, a comparison between the pull-in instability results of MADM and the previous studies is performed. Consider a typical microbeam with the following geometrical dimensions and material properties: $E=$ 169 Gpa, $v=$ 0.06, $w=$ 50 μm, $t=$ 3 μm. Two values of $L=$ 250 μm and $L=350$ μm are also adopted for the length of the microbeam. Table 2 shows a comparison between pull-in voltages obtained by eight terms of MADM, numerical method and the results reported in the literature [36,53]. As seen, the results of the present study are in very good agreement with the previous studies.

It is noteworthy that at the onset of pull-in instability there is not any solution for deflection of nanobeam (i.e. $g(x)$), and hence, the $g(x)$ diverges. Pull-in is the point which the elastic restoring force (right hand side of Eq. (10)) can no longer balance the external forces (Left hand side of Eq. (10)). Further increasing the forces (i.e. commonly voltage) would cause the structure to have a dramatic displacement jump which causes the structure collapse [54]. In addition, because of the symmetry of the nanobeam, the maximum deflection at the onset of pull-in instability occurs at $x=0.5$. The parameters and variables at the onset of pull-in instability are denoted by subscript of PI.

4. Results and discussion

4.1. Eta behavior and validation

The governing mid-plan stretching equation of the nanobeam, which is a function of Casimir, voltage and liquid Layer parameters, is solved using MADM in previous section. The results show that governing equation diverges for high values of η where $\eta=6(H/t)^2$. Abdel Rahman et al. [12] have analyzed the pull-in instability of dry micro switches and they considered the mid-plane stretching effects. In the case of $\alpha=K=0$, the present study reduces to the work of Abdel Rahman et al. [12]. Fig. 4 shows the effect of η on the maximum deflection of beam for different values of β. Moreover, in this figure, MADM and Numerical results, obtained in the present work, are compared with the work of Abdel Rahman et al. [12] and found in good agreement. The outcomes indicate that high values of η induce the divergence of the governing equation before pull-in instability. Therefore, the small values of η parameter (Preferably smaller than 10) were found adequate to analyze the pull-in instability of nanoswitches using mid-plane stretching model [12].

Based on the work of Fruehling et al. [55], the dimensions of a practical nanobeam can be adopted as $L=1050$ nm, $w=200$ nm, $H=20$ nm, $t=50$ nm. In the present study, these dimensions are used to evaluate the practical ratios (H/w) and $6(H/t)^2$, which

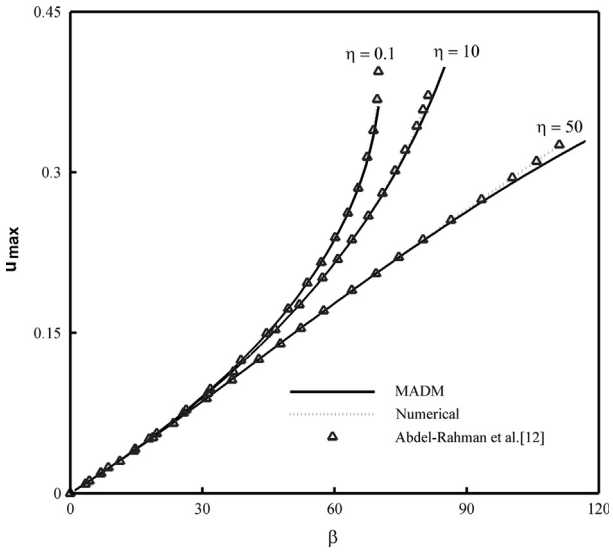

Fig. 4. The effect of η on the pull-in voltage parameter.

yields $H/w=0.1$ and $6(H/t)^2=0.96$. For a specified nanoswitch, the parameters of η and H/w can be considered as a constant, and hence, the fringing field parameter only depends on the voltage parameter. The voltage parameter (β) can be changed by changing the applied voltage difference between nanoswitch electrodes (i.e. nanobeam and substrate). The remaining parameters (i.e. α, K) can be considered variable because of changing in the size of the nanobeam. Using these assumptions, the pull-in stability of the nanobeam is a function of the three remaining non-dimensional parameters of voltage (β), Casimir (α) and liquid layer (K). These assumptions reduce the number of non-dimensional parameters without losing the generality of the solution. Therefore, in the following text, the values of η and H/w are assumed as $\eta=0.96$, and $H/w=0.1$ for convenience.

4.2. Parameters behavior

In this section, the influence of three important non-dimensional parameters of the applied voltage parameter (β), liquid layer parameter (K) and Casimir parameter (α) and their simultaneous effects on the pull-in instability of nanoswitches is examined. It is worth noticing that the applied voltage parameter (β) indicates the applied force because of the electrical attraction. Likewise, the Casimir parameter (α) indicates the induced force because of the Casimir effects. Therefore, from the practical point of view, the pull-in values of these parameters, i.e. (α_{PI}) and (β_{PI}), indicate the corresponding required forces which induce the pull-in instability of the nanoswitch. In addition, the pull-in value of the liquid layer parameter (K) indicates the corresponding liquid layer in which the pull-in instability occurs [10].

In order to find the pull-in value of each non-dimensional parameter, first it is needed that the other two parameters take predefined values. For example, for fixed values of K and α, the pull-in value of β can be obtained from the solution of Eq. (10) by increase of β until the pull-in instability occurs. Then, the set of K, α and the obtained value of β shows a set of pull-in parameters. In addition, the variation range, which a parameter can be changed before pull-in instability occurs, also is important in practical design of nanoswitches. It is clear that the magnitudes of the non-dimensional parameters induce direct influence on the pull-in value of the other parameter. In order to find the maximum pull-in value of voltage parameter, the other parameters, i.e. K and α, should be taken as zero [10]. Here, the following equation, Eq. (17.a), leads to the maximum value of the non-dimensional

applied voltage parameter:

$$\frac{\partial^4 g}{\partial x^4} = \eta \int_0^1 \left(\frac{dg}{dx}\right)^2 dx \times \frac{\partial^2 g}{\partial x^2} - \frac{\beta}{g(x)^2} - \frac{\gamma_{fr}}{g(x)} \tag{17.a}$$

Similarly, Eq. (17.b) can be utilized to obtain the maximum value of pull-in instability for Casimir parameter.

$$\frac{\partial^4 g}{\partial x^4} = \eta \int_0^1 \left(\frac{dg}{dx}\right)^2 dx \times \frac{\partial^2 g}{\partial x^2} - \frac{\alpha}{g(x)^4} \tag{17.b}$$

Eq. (17.a) neglects the effect of Casimir parameter and solely shows the effect of voltage parameter on the deflection of nanobeam. Eq. (17.b) neglects the electrostatic forces and shows the effect of Casimir parameter on the deflection of the beam. In the following figures, the points A and B indicate the results obtained from Eqs. (17.a) and (17.b), respectively.

Fig. 5 shows the effect of the pull-in voltage parameter on the Casimir parameter for selected values of liquid layer parameter at the onset of pull-in instability. This figure reveals that decrease of the pull-in voltage parameter increases the required value of Casimir parameter. As seen, the minimum value of required pull-in voltage parameter occurs at the Pint B. This observation is in good agreement with physic of the nanobeams; because the presence of an external force reduces the required voltage for pull-in instability. In addition, an increase of liquid layer parameter leads to negative value of $K(1-\varepsilon_f)$ in Eq. (10.a) and hence decreases the pull-in voltage. It is worth noticing that the magnitude of ε_f always is greater than unit, and hence, the value of $K(1-\varepsilon_f)$ is always lower than zero which indicates the minus effects. The presence of Casimir force and liquid layer, which are appeared in Eq. (10.a), represent different physical insights. The Casimir parameter indicates the presence of an external force, but the liquid layer parameter indicates the resistance in electrical force of acting on the nanobeam.

Fig. 6 shows the simultaneous effect of Casimir and liquid layer parameters on the pull-in voltage parameter. As mentioned, the points of A and B depict the solution of Eqs. (17.a) and (17.b), respectively. The results of Fig. 6 in agreement with Fig. 5 depict that an increase of the Casimir parameter would decrease the required pull-in voltage at the onset of pull-in instability. Interestingly, this figure shows that the decrease of liquid layer parameter increases the influence of Casimir parameter on the non-dimensional pull-in voltage. As the Casimir parameter increases to 39, the pull-in voltage parameter decreases to zero.

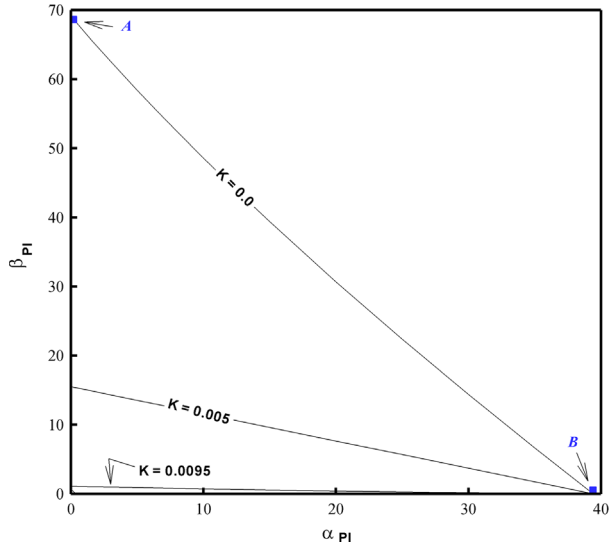

Fig. 5. The effect of liquid layer parameter on the pull-in Casimir parameter.

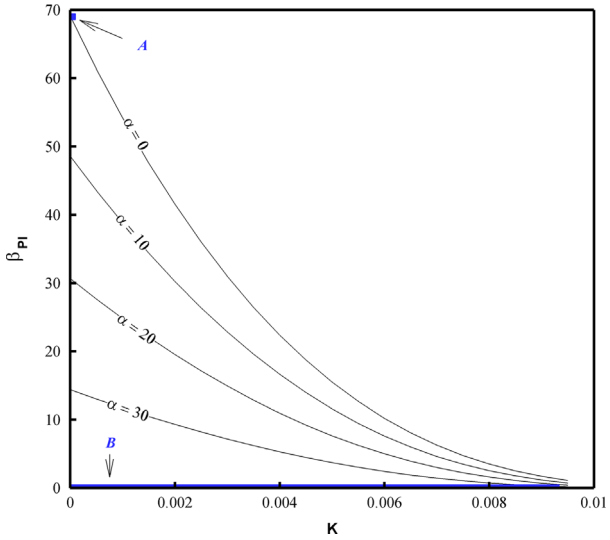

Fig. 6. The effect of Casimir and liquid layer parameters on the pull-in voltage parameter.

Further increase of Casimir parameter more than 39 induces pull-in instability, even in the absence of any external voltage. Fig. 6 obviously shows that an increase of Casimir parameter would decrease the effect of the voltage parameter.

4.3. 4.3 Balanced liquid layer

In this section, the effect of non-dimensional liquid layer parameter on the pull-in deflection of nanobeam will be analyzed; the balanced liquid layer value which is the main outcome of the present study will be introduced.

In order to analyze the effect of the liquid layer parameter (K) on the pull-in instability of the nanoswitch, the practical range of this parameter should be analyzed. Based on the definition of liquid layer parameter in Eq. (9), this parameter can be changed from zero (zero thickness of the liquid) to the value of $1/\varepsilon_f$ (when the gap is filled with the liquid). Hence, for the water, the maximum value of liquid layer is $K=1/80.1$ (or $K=0.0125$). However, physically, the thickness of the liquid layer is much lower than the gap between the beam and substrate. Therefore, in the present study, the range of $0<K<0.0095$ is adopted for analysis of the liquid layer parameter. It is worth noticing that the increase of liquid layer parameter decreases the pull-in voltage parameter (as seen in Figs. 5 and 6). Here, using the following relation, the effect of liquid layer parameter on the pull-in voltage and pull-in deflection of nanobeam is examined:

$$\frac{\partial^4 g}{\partial x^4} = \eta \int_0^1 \left(\frac{dg}{dx}\right)^2 dx \times \frac{\partial^2 g}{\partial x^2} - \frac{\beta}{(-0.75145+g(x))^2} - \frac{\gamma_{fr}}{g(x)} \tag{17.c}$$

Eq. (17.c) neglects the Casimir force and models a nanobeam with a layer of water ($K=0.0095$). The value of -0.75145 in Eq. (17.c) comes from the relation of $K(1-\varepsilon_f)$ where ε_f is the relative permeability of water ($\varepsilon_f=80.1$). In the following figures, the point C indicates the results obtained from Eq. (17.c).

Fig. 7 depicts the effect of the liquid layer parameter on the pull-in deflection of the nanobeam. This figure reveals that there are three distinct trend of behavior for variation of pull-in deflection with increase of Casimir parameter. For the liquid layer parameter which its magnitude is less than 0.005, an increase of the Casimir parameter would decrease the pull-in deflection. By contrast, for the values of liquid layer parameter higher than 0.005, the effect of the Casimir parameter on the pull-in deflection is inverted. In this case, an increase

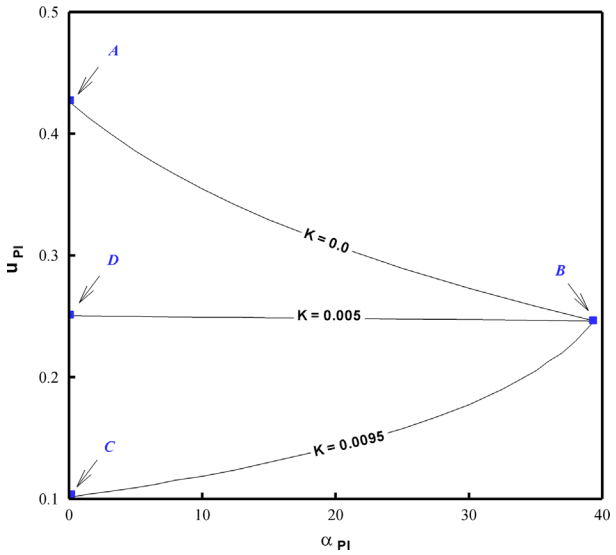

Fig. 7. The effect of Casimir parameter and liquid layer parameter on the maximum pull-in deflection of the nanobeam.

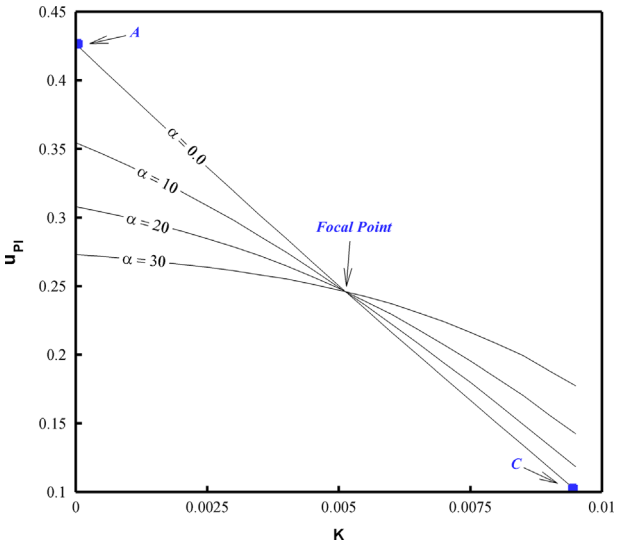

Fig. 8. Balance liquid layer of nanobeam for maximum deflection.

of the Casimir parameter would also increase the maximum deflection (beam deflection) at the onset of pull-in instability. For liquid layer parameter of $K=0.005$, the variation of Casimir parameter does not have any significant effect on the pull-in deflection. The reason for these three distinct behaviors of pull-in deflection can be discussed as follow:

In the case of solely electrical force (Eqs. (17.a) and 17.c)), the magnitudes of non-dimensional deflections for $K=0$ and $K=0.0095$ are $u_{PI}=0.43$ and $u_{PI}=0.1$, respectively; while the pull-in deflection for solely Casimir force, neglecting the voltage effects (Eq. (17.b)), is $u_{PI}=0.25$. Therefore, by increasing the Casimir effect, the non-dimensional pull-in deflection tends to move from $u_{PI}=0.43$ (solely electrical force/point, A) to $u_{PI}=0.25$ (solely Casimir force/point, B). However, in the case of $K=0.0095$, the corresponding pull-in deflection of solely electrical force (point C, $u_{PI}=0.1$) is lower than that of the solely Casimir force ($u_{PI}=0.25$). Therefore, increase of Casimir effects increases the pull-in deflection. The value of the pull-in deflection $u_{PI}=0.25$ on the AC segment is labeled as point D. Point D shows the pull-in deflection of a nanobeam with $K=0.005$ and neglecting the Casimir effects, i.e. $\alpha=0$. Therefore, in the case of $K=0.005$, the corresponding pull-in deflection of electrical force (point D, $u_{PI}=0.25$) and solely Casimir force (point B, $u_{PI}=0.25$) are equal. Hence, increasing the Casimir effects transfers the pull-in deflection from $u_{PI}=0.25$ to $u_{PI}=0.25$ which is the straight line in the Fig. 7. Hence, for the liquid layer parameter of $K=0.005$, the beam deflection is independent of the Casimir effects. This interesting value of liquid parameter is introduced as Balance Liquid Layer (BLL) which is denoted by K^*. The magnitude of pull-in deflection at segment D-B shows the corresponding non-dimensional pull in deflection of the nanobeam for the value of BLL, i.e. $K^* \approx K = 0.005$. Fig. 7 obviously shows that the segment D–B is a horizontal line which has the unique pull-in deflection of 0.25.

Fig. 8 shows the non-dimensional deflection of nanobeams for selected values of Casimir parameter and a range of liquid layer parameter (K between 0 and 0.0095). The segment D–B, which was a line in Fig. 7, reduces to a point in Fig. 8. This point is a focal point plotted in Fig. 8. The value of liquid layer parameter of the focal point in Fig. 8 introduces the value of balance liquid layer for pull-in deflection of a typical nanobeam. This focal point shows that there is a distinct liquid-layer parameter, in which the variation of the dimensionless Casimir parameter does not have a significant influence on the values of pull-in deflection. The focal point was defined as balance liquid layer. The balance liquid layer

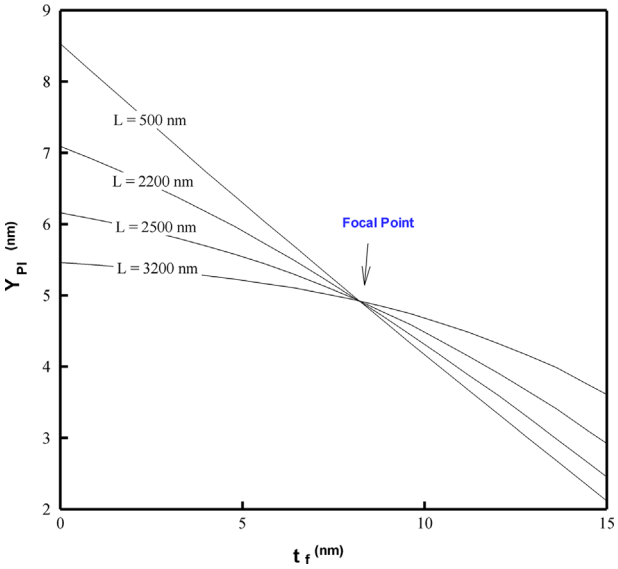

Fig. 9. The effect of the liquid layer thickness on the absolute value of the maximum deflection of the nanobeam with $w=200$ nm, $H=20$ nm and $t=50$ nm.

phenomenon occurs because the nanobeam is subject to the simultaneous effects of liquid layer and Casimir force.

For a practical case, consider a nanobeam in which the thickness and the width of the electrode are 50 nm and 200 nm, respectively; the gap between the electrode and the substrate is 20 nm. There is a layer of water beneath the beam with thickness of t_f where the relative permeability of water is 80.1. Length of the beam is selected as a free parameter. For this practical nanoswitch, the pull-in deflection of the beam (Y_{PI}) as a function of water layer thickness (t_f) is plotted in the Fig. 9. The results are also depicted for different lengths of the beam. As seen, when the water layer thickness is 8 nm, the pull-in deflection of the nanobeam adopts the fixed deflection of 5 nm, and the variation of the length of the nanobeam does not affect the pull-in deflection.

4.4. Stress treatment

Stress analysis of nanoswitches is important for controlling the mechanical properties of materials [13] and preventing the failure

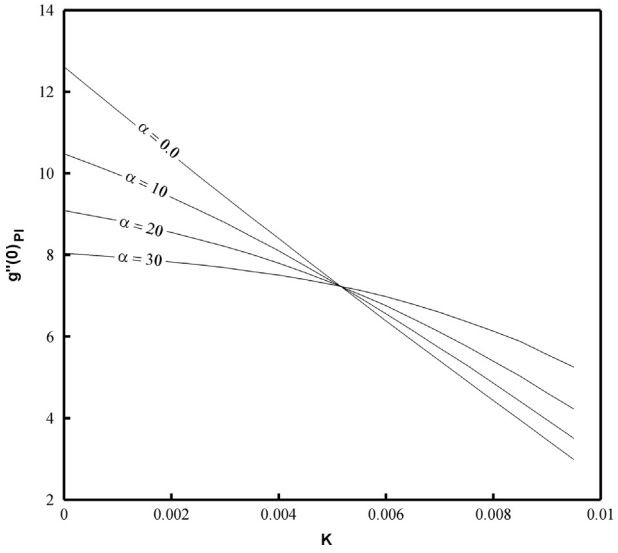

Fig. 10. Balance liquid layer of nanobeam for maximum momentum.

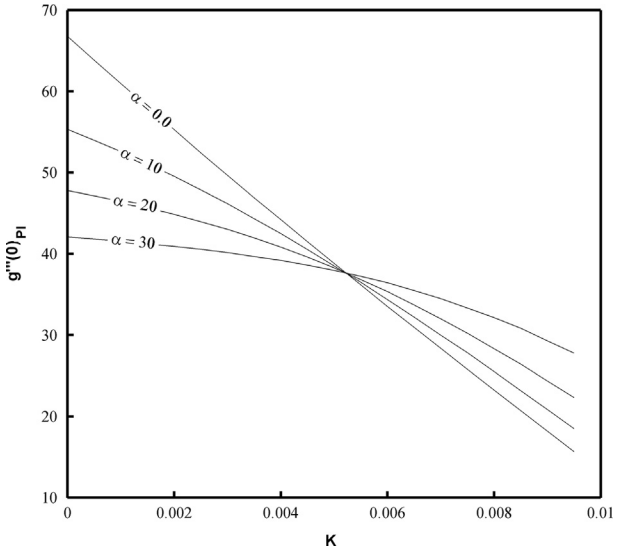

Fig. 11. Balance liquid layer of nanobeam for maximum shear force.

of the switch. As known, the maximum bending moment and shear force occur in the boundary end points of a fixed–fixed type beam with uniform cross section of area [43]. Considering the von Karman formula in the axial strain relationship, the maximum internal stress resultants at an arbitrary cross-section of the nanobeam are defined as [56,57],

$$\sigma_{xx} = htE_{eff}/(2L^2) \times g''(x) + t^2E_{eff}/(2L^2) \times T^* \quad (18.a)$$

$$\tau_{xy} = -ht^2E_{eff}/(8L^3) \times (g'''(x) - g'(x) \times T^*) \quad (18.b)$$

Considering the definition of new constants as below,

$$\sigma_0 = htE_{eff}/(2L^2) \quad (19.a)$$

$$\tau_0 = ht^2E_{eff}/(8L^3) \quad (19.b)$$

the maximum pull-in internal stress resultants at the initial cross-section of the nanobeam are calculated as

$$\sigma_{PI} = \sigma_0 \times (g''_{PI}(0) + 2.5T^*_{PI}) \quad (20.a)$$

$$\tau_{PI} = \tau_0 \times g'''_{PI}(0) \quad (20.b)$$

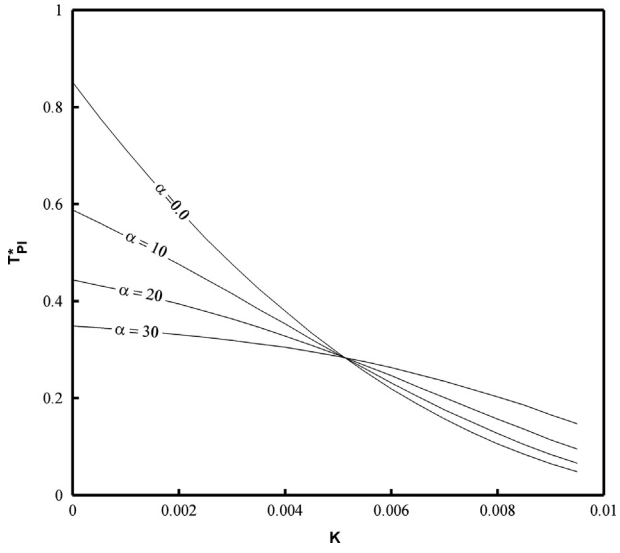

Fig. 12. Balance liquid layer of nanobeam for stretching force.

Table 3
Maximum deflection, shear force, bending momentum and stretching in Pull-in situation of nanobeam at balance liquid layer.

Fig. 10		Fig. 11		Fig. 12	
K^*	$g''(0)_{PI}$	K^*	$g'''(0)_{PI}$	K^*	T^*_{PI}
0.00515	7.21	0.00521	37.6	0.00513	0.284

where σ_{PI} is the maximum normal stress and τ_{PI} is the maximum shear stress at the initial cross-section of the nanobeam. σ_0 and $\tau_0$are constants utilized to simplifying the stresses relations.

Figs. 10–12 show the simultaneous effects of the liquid layer parameter on the values of the $g''(0)_{PI}$, $g'''(0)_{PI}$ and T^*_{PI}, respectively. It can be observed that the values of BLL (focal points) in the Figs. 10–12 are not identical. Therefore, the corresponding values of K^* for the pull-in deflection, shear force, bending moment and stretching are shown in Table 3. The results of this table reveals that the values of K^* are very close to each other; however they are not identical.

These values of BLL parameters are of interest for design of nanoswitches. Designing a nanoswitch with the BLL parameter diminishes the effect of Casimir parameter on the pull-in deflection and internal stress resultants of the beam. Diminishing the effect of Casimir parameter also decreases the non-linearity of the beam deflection. A nanobeam with less non-linearity is more suitable for practical applications.

5. Summary and conclusions

In this paper, the pull-in instability of an electrostatic doubly clamped nanobeam in the presence of a liquid layer and Casimir force is investigated. The modified Adomian decomposition method is successfully utilized to obtain the pull-in instability of nanobeam. From comparison between analytical results and numerical results it is evident that the eight terms of Adomian series (i.e. x^{28}) provides sufficient accuracy for the analytical calculations. In the present model, the liquid layer parameter indirectly affects the pull-in value of Casimir parameter. Actually, the presence of liquid layer affects the electrostatic force, and consequently, it affects the pull-in value of Casimir parameter.

It is found that there is a specific value of liquid layer parameter in which the variation of Casimir parameter does not have a significant effect on the pull-in deflection of nanobeam. This value of liquid layer parameter is introduced as Balanced Liquid Layer (BLL). The values of BLL for pull-in shear force, bending moment and stretching of nanobeam are obtained. The results of present study can be summarized as follows:

(1) The increase of Casimir parameter decreases the required pull-in voltage.
(2) The increase of liquid layer parameter decreases the value and the rage of pull-in voltage.
(3) For each of the important design parameters such as pull-in deflection, shear force and bending moments and stretching of the nanobeam always there is a value of balance liquid parameter (BLL) in which the variation of that design parameter is independent of Casimir effects.

The Balanced Liquid Layer (BLL) is a unique value of non-dimensional liquid layer which has been determined by analyzing a massive combination of the pull-in data. Obtaining BLL using experimental test is very time-consuming and expensive. Thus, there is not any experimental analysis considering the BLL. However, there are reports [33] on the effect of the presence of a water layer underneath of nanoswitches which strongly affects their pull-in instability. In the present study, the value of BLL has been obtained theoretically for the first time. The present value of BLL can provide a basis for running direct experimental tests in order to find the experimental value of this parameter. By using the BLL value, designing an array of nanoswitches with different lengths but equal pull-in deflections is possible. The calculated values of BLL can be very useful in design of wet nanobeams in the applications in which the presence of Casimir effects is common, and they affect the performance of the device. Designing a nanobeam with the dimension and physical parameters, which the non-dimensional liquid layer parameter of the nanobeam is near the BLL point, can significantly decrease the effect of Casimir force.

Acknowledgments

The authors are grateful to Shahid Chamran University of Ahvaz for its crucial support.

Appendix A

Based on the modified Adomian decomposition method, the inverse operator $L^{-(i)}$ is defined as an i-fold integral operator as [36]:

$$L^{-(i)}=\underbrace{\int_0^x\int_0^x\ldots\int_0^x(.)dx\ldots dxdx}_{i\ \text{integral}\ \ term}, \tag{A.1}$$

to obtain a solution for the following mid-plan stretching equation of the beam:

$$\frac{d^4g}{dx^4}-T^*\frac{d^2g}{dx^2}=N(g(x)), \tag{A.2}$$

Here, T^* is considered as an unknown constant, and $N(g(x))$ is a non-linear function. Applying the inverse operator $L^{-(4)}$ to both sides of Eq. (9) leads to

$$g(x)=d_0+d_1x+\frac{1}{2}d_2x^2+\frac{1}{6}d_3x^3+T^*\times L^{(-2)}(g(x))+L^{(-4)}(N(g(x))), \tag{A.3}$$

Now, the non-linear function $N(g(x))$ in Eq. (A.2) is approximated by series of Adomian polynomials as:

$$N(g(x))=\sum_{n=0}^{\infty}N_n, \tag{A.4}$$

and also, $g(x)$ is defined by series as:

$$g(x)=\sum_{n=0}^{\infty}g_n, \tag{A.5}$$

Substituting Eq. (A.4) and (A.5) into Eq. (A.3), the recursive relation of the $g(x)$ can be generally shown as [58]:

$$\sum_{n=0}^{\infty}g_n=d_0+d_1x+\frac{1}{2}d_2x^2+\frac{1}{6}d_3x^3+T^*\times L^{-(2)}\left(\sum_{n=0}^{\infty}g_{n-1}\right)+L^{-(4)}\left(\sum_{n=0}^{\infty}N_{n-1}\right) \tag{A.6}$$

The recursive relations for Modified Adomian Decomposition method are as follows [58]:

$$g_0=d_0, \tag{A.7}$$

$$g_1=d_1x+\frac{1}{2}d_2x^2+\frac{1}{6}d_3x^3+T^*\times L^{-(2)}(g_0)+L^{-(2)}(N_0), \tag{A.8}$$

$$g_k=T^*\times L^{-(2)}(g_{k-1})+L^{-(4)}(N_{k-1}), \tag{A.9}$$

The Adomian polynomial N_n is derived by the following convenient equations [18]:

$$N_n=\sum_{v=1}^{n}C(v,n)H_v(g_0),\quad (n>0), \tag{A.10}$$

$$C(v,n)=\sum_{p_i}\prod_{i=1}^{v}\frac{g_{pi}^{ki}}{k!},\quad \left(\sum_{i=1}^{v}k_ip_i=n,0\le i\le n,1\le p_i\le n-v+1\right), \tag{A.11}$$

$$H_v(g_0)=d^v/dg_0{}^v[N(g_0)], \tag{A.12}$$

where k_i is the number of repetition in g_{pi} and the values of p_i are selected from the above range by combination without repetition. The constants d_0-d_4 will be calculated by applying boundary conditions Eqs. (10-b) and (10-c).

Appendix B.1

The Adomian polynomials are derived as,

$$A_0=\frac{1}{g_0{}^4},\quad B_0=\frac{1}{(K'+g_0)^2},\quad C_0=\frac{1}{g_0}, \tag{B.1}$$

$$A_1=g_1H_1(g_0)=-\frac{4g_1}{g_0{}^5},\quad B_1=-\frac{2g_1}{(K'+g_0)^3},\quad C_1=-\frac{g_1}{g_0{}^2}, \tag{B.2}$$

$$A_2=g_2H_1(g_0)+\frac{1}{2!}g_1^2H_2(g_0)=-\frac{4g_2}{g_0{}^5}-\frac{10g_1{}^2}{g_0{}^6},$$
$$B_2=-\frac{2g_2}{(K'+g_0)^3}-\frac{3g_1{}^2}{(K'+g_0)^4},$$
$$C_2=\frac{g_2}{g_0{}^2}+\frac{g_1{}^2}{g_0{}^3}, \tag{B.3}$$

where A_n, B_n and C_n are the Adomian polynomials of $1/g(x)^4$, $1/(K'+g(x))^2$ and $1/g(x)$, respectively.

Appendix B.2

Considering $N(g(x))=\alpha\times A_n+\beta\times B_n+\ \gamma_{fr}\times C_n$, letting $g_0=1$ and inserting Eq. (B.1) into Eq. (A.8) leads to:

$$g_1(x)=\frac{1}{2}d_2x^2+\frac{1}{6}d_3x^3+T^*\frac{x^2}{2}-\left(\alpha+\frac{\beta}{(1+K^*)^2}+\gamma_{fr}\right)\frac{x^4}{24}, \tag{B.4}$$

Substituting Eq. (B.2) into Eq. (A.9) yields:

$$\begin{aligned}g_2(x)=&\frac{T^*d_2+T^{*2}}{24}x^4+\frac{T^*d_3}{120}x^5\\&+\left(\frac{\alpha d_2}{180}+\frac{\alpha T^*}{240}+\frac{\beta d_2}{360(1+K^*)^3}+\frac{\gamma_{fr}d_2}{720}-\frac{T^*\beta}{720(1+K^*)^2}\right.\\&\left.+\frac{T^*\beta}{360(1+K^*)^3}\right)x^6+\left(\frac{\alpha d_3}{1260}+\frac{\beta d_3}{2520(1+K^*)^3}+\frac{\gamma_{fr}d_3}{5040}\right)x^7\\&-\left(\frac{\gamma_{fr}\alpha_4}{8064}-\frac{\gamma_{fr}\beta}{20160(1+K^*)^3}-\frac{\gamma_{fr}\beta}{40320(1+K^*)^2}\right.\\&-\frac{\beta\alpha}{20160(1+K^*)^3}-\frac{\beta\alpha}{10080(1+K^*)^2}-\frac{\alpha^2}{10080}\\&\left.-\frac{\beta^2}{20160(1+K^*)^5}-\frac{{\gamma_{fr}}^2}{40320}\right)x^8\end{aligned} \tag{B.5}$$

References

[1] R.C. Batra, M. Porfiri, D. Spinello, Review of modeling electrostatically actuated microelectromechanical systems, Smart Materials and Structures 16 (2007) R23–R31.

[2] J. Wu, G.K. Fedder, L.R. Carley, A low-noise low-offset capacitive sensing amplifier for a 50-μg/√Hz monolithic CMOS MEMS accelerometer, IEEE Journal of Solid-State Circuits 39 (5) (2004) 722–730.

[3] A. Loui, F.T. Goericke, T.V. Ratto, J. Lee, B.R. Hart, W.P. King, The effect of piezoresistive microcantilever geometry on cantilever sensitivity during surface stress chemical sensing, Sensors and Actuators A 147 (2008) 516–521.

[4] C. Ke, H.D. Espinosa, In situ electron microscopy electromechanical characterization of a bistable NEMS device, Small 2 (2006) 1484–1489.

[5] S.L. Miller, M.S. Rodgers, G.L. Vigne, J.J. Sniegowski, P. Clews, D.M. Tanner, K. A. Peterson, Failure modes in surface micromachined microelectromechanical actuation systems, Microelectronics Reliability 39 (1999) 1229–1237.

[6] J.S. LEE, Mechanics of Nanoscale Beams in Liquid Electrolytes: Beam Deflections, Pull-in Instability, and stiction, Doctor of Philosophy, Aerospace Engineering, Texas A&M University, 2008.

[7] S.N. Cha, J.E. Jang, Y. Choi, G.A.J. Amaratunga, D.J. Kang, et al., Fabrication of a nanoelectromechanical switch using a suspended carbon nanotube, Applied Physics Letters 86 (2005) 083105.

[8] J. Cheng, J. Zhe, X. Wu, Analytical pull-in study on non-deformable electrostatic micro actuators. In: Technical Proceedings of the 2002 International Conference on Modeling and Simulation of Microsystem, 2002, ISBN: 0-9708275-7-1, pp. 287–290.

[9] S. Gorthi, A. Mohanty, A. Chatterjee, Cantilever beam electrostatic MEMS actuators beyond pull-in, Journal of Micromechanics and Microengineering 16 (2006) 1800–1810.

[10] E. Yazdanpanahi, A. Noghrehabadi, M. Ghalambaz, Balance dielectric layer for micro electrostatic switches in the presence of capillary effect, International Journal of Mechanical Sciences 74 (2013) 83–90.

[11] A.S. Rollier, B. Legrand, D. Collard, L. Buchaillot, stability and pull-in voltage of electrostatic parallel-plate actuators in liquid solutions, Journal of Micromechanics and Microengineering 16 (2006) 794–801.

[12] M.E. AbdelRahman, M.I. Younis, A.H. Nayfeh, Characterization of the Mechanical Behavior of an Electrically Actuated Microbeam, Journal of Micromechanics and Microengineering 12 (2002) 759–766.

[13] A. Soroush, A. Koochi, A.S. Kazemi, A. Noghrehabadi, H. Haddadpour, M. Abadyan, Investigating the effect of Casimir and van der Waals attractions on the electrostatic pull-in instability of nano-actuator, Physica Scripta 82 (2010) 045801.

[14] A. Koochi, A. Noghrehabadi, M. Abadyan, E. Roohi, Investigation of the effect of van der Waals force on the instability of electrostatic nano-actuators, International Journal of Modern Physica B 25 (2011) 3965–3976.

[15] A. Noghrehabadi, M. Ghalambaz, A. Ghanbarzadeh, A new approach to the electrostatic pull-in instability of nanocantilever actuators using the ADM–Padé technique, Computers & Mathematics with Applications 64 (2012) 2806–2815.

[16] N.J. Israelachvili, Intermolecular and Surface Forces, Academic Press, London, 1992.

[17] S.K. Lamoreaux, The Casimir force: background, experiments, and applications, Reports on Progress in Physics 68 (2005) 201–236.

[18] W.H. Lin, Y.P. Zhao, Dynamic behavior of nanoscale electrostatic actuators, Chinese Physics Letters 20 (2003) 2070–2073.

[19] A. Gusso, G.J. Delben, Dispersion force for materials relevant for micro and nanodevices fabrication, Journal of Physics D, Applied Physics 41 (175405) (2008) 11.

[20] A. Koochi, A. SadatKazemi, Y. TadiBeni, A. Yekrangi, M. Ababdyan, Theoretical study of the effect of Casimir attraction on the pull-in behavior of beam-type NEMS using modified Adomian method, Physica E 43 (2010) 625–632.

[21] F.M. Serry, D. Walliser, G.J. Maclay, The role of the casimir effect in the static deflection and stiction of membrane strips in microelectromechanical systems (MEMS), Journal of Applied Physics 84 (1998) 2501–2506.

[22] W.H. Lin, Y.P. Zhao, Non-linear behavior for nanoscale electrostatic actuators with Casimir force, Chaos Solitons and Fractals 23 (2005) 1777–1785.

[23] A. Ramezani, A. Alasty, J. Akbari, Closed-form solutions of the pull-in instability in nano-cantilevers under electrostatic and intermolecular surface forces, International Journal of Solids and Structures 44 (2007) 4925–4941.

[24] A. Ramezani, A. Alasty, Combined action of Casimir and electrostatic forces on nanocantilever arrays, Acta Mechanica 212 (2010) 305–317.

[25] A. Noghrehabadi, M. Eslami, M. Ghalambaz, Influence of size effect and elastic boundary condition on the pull-in instability of nano-scale cantilever beams immersed in liquid electrolytes, International Journal of Non-Linear Mechanics 52 (2013) 73–84.

[26] M. Ghalambaz, A. Noghrehabadi, M. Abadyan, Y.T. Beni, A.N. Abadi, M.N. Abadi, A new power series solution on the electrostatic pull-in instability of nano cantilever actuators, Procedia Engineering 10 (2011) 3708–3716.

[27] A. Noghrehabadi, M. Ghalambaz, A. Ghanbarzadeha, Buckling of multi wall carbon nanotube cantilevers in the vicinity of graphite sheets using monotone positive method, Journal of Computational and Apllied Research in Mechanical Engineering 1 (2012) 89–97.

[28] A. Noghrehabadi, Y.T. Beni, A. Koochi, A. Kazemi, A. Yekrangi, M. Abadyan, M.N. Abadi, Closed-form approximations of the pull-in parameters and stress field of electrostatic cantilevers nano-actuators considering van der Waals attraction, Procedia Engineering 10 (2011) 3750–3756.

[29] A. Noghrehabadi, M. Ghalambaz, Y.T. Beni, M. Abadyan, M.N. Abadi, M. N. Abadi, A new solution on the buckling and stable length of multi wall carbon nanotube probes near graphite sheets, Procedia Engineering 10 (2011) 3725–3733.

[30] G. Adomian, A Review of the Decomposition Method in Applied Mathematics, Journal of Mathematical Analysis and Applications 135 (1988) 501–544.

[31] A.M. Wazwaz, A reliable modification of Adomian decomposition method, Applied Mathematics and Computation 102 (1999) 77–86.

[32] J.S. Duan, T. Chaolu, R. Rach, Solutions of the initial value problem for non-linear fractional ordinary differential equations by the Rach-Adomian-Meyers modified decomposition method, Applied Mathematics and Computation 218 (2012) 8370–8392.

[33] J.S. Duan, R. Rach, New higher-order numerical one-step methods based on the Adomian and the modified decomposition methods, Applied Mathematics and Computation 218 (2012) 2810–2828.

[34] J.S. Duan, R. Rach, Higher-order numeric Wazwaz-El-Sayed modified Adomian decomposition algorithms, Applied Mathematics and Computation 63 (2012) 1557–1568.

[35] R. Rach, J.S. Duan, Near-field and far-field approximations by the Adomian and asymptotic decomposition methods, Applied Mathematics and Computation 217 (2011) 5910–5922.

[36] J.H. Kuang, C.J. Chen, Adomian decomposition method used for solving nonlinear pull-in behavior in electrostatic micro-actuators, Mathematical and Computer Modelling 41 (2005) 1479–1491.

[37] M.R. Abadyan, Y.T. Beni, A. Noghrehabadi, Investigation of elastic boundary condition on the pull-in instability of beam-type NEMS under van der Waals attraction, Procedia Engineering 10 (2011) 1724–1729.

[38] A. Koochi, A.S. Kazemi, A. Noghrehabadi, A. Yekrangi, M. Abadyan, New approach to model the buckling and stable length of multi walled carbon nanotube probes near graphite sheets, Materials and Design 32 (2011) 2949–2955.

[39] H.M. Ouakad, M.I. Younis, modeling and simulations of collapse instabilities of microbeams due to capillary forces, Mathematical Problems in Engineering (2009) (2009) 16. (Article ID 871902).

[40] G. Palasantzas, V.B Svetovoy, P.J VanZwol, Influence of ultrathin water layer on the van der Waals/Casimir force between gold surfaces, Physical Review 79 (2009) 235434.

[41] P.A. Thiel, TE. Madey, the interaction of water with solid surfaces: fundamental aspects, Surface Science Reports 7 (1987) 211–385.

[42] Y. Hayamizu, T. Yamada, K. Mizuno, R.C. Davis, D.N. Futaba, M. Yumura, K. Hata, Integrated three-dimensional microelectromechanical devices from processable carbon nanotube wafers, Nature Nanotechnology 3 (2008) 289–294.

[43] S. Timoshenko, Theory of Plates and Shells, McGrawHill, NewYork, 1987.

[44] Y. Zhang, Y. Zhao, Static study of cantilever beam stiction under electrostatic force influence, Acta Mechanica Solida Sinica 17 (2004) 104–112.

[45] R. Legtenberg, H.A.C. Tilmans, J. Elders, M Elwenspoek, Stiction of surface micromachined structures after rinsing and drying: model and investigation of adhesion mechanisms, Sensor Actuator A 43 (1994) 230–238.

[46] F.P. Beer, J.H. Johnston, J.T. Dewolf, D.F. Mazurek, Mechanics of Material, 5th ed., Mc-Graw Hill Companies, New York, 2009.

[47] R. Garg, Analytical and Computational Methods in Electromagnetics, Artech House, Boston/London, 2008.

[48] K. Chen, J.W. Zhang, Comparison of the RF MEMS switches with dielectric layers on the bridge's lower surface and on the transmission line, Science China Information Sciences 54 (2011) 396–406.
[49] G. Palasantzas, P.J. Van Zwol, J Th.M. De Hosson, Transition from Casimir to van der Waals Force between Macroscopic Bodies, Applied Physics Letters 93 (2008) 1219121–1219123.
[50] R. Esquivel Sirvent, L. Reyes, J. Barcenas, Stability and the proximity theorem in casimir actuated nano devices, New Journal of Physics 8 (2006) 241.
[51] M. Bordag, U. Mohideen, V.M. Mostepanenko, New developments in the Casimir effect, Physics Reports 353 (2001) 1–205.
[52] E. Fehlberg, Low-order classical Runge-Kutta formulas with step size control and their application to some heat transfer problems, NASA Technical Report 3, 1969.
[53] P.M. Osterberg, S.D. Senturia, M-TEST: a test chip for MEMS material property measurement using electrostatically actuated test structures, Journal of Microelectromechanical Systems 6 (1997) 107–118.
[54] Y. Zhang, Y.P. Zhao, Numerical and analytical study on the pull-in instability of micro-structure under electrostatic loading, Sensors and Actuators A 127 (2006) 366–380.
[55] A. Fruehling, Sh. Xiao, M. Qi, K. Roy, Peroulis D. Nano-switch for Study of Gold Contact Behavior. In: IEEE Sensors 2009 Conference, Birck Nanotechnology Center, Purdue University, 2009, 247–251.
[56] Y. Fu, J. Zhang, Y. Jiang, Influences of the surface energies on the non-linear static and dynamic behaviors of nanobeams, Physica E 42 (2010) 2268–2273.
[57] S. Chaterjee, G. Pohit, A large deflection model for the pull-in analysis of electrostatically actuated microcantilever beams, Journal of Sound and Vibration 322 (2009) 969–986.
[58] A.M. Wazwaz, A reliable algorithm for solving boundary value problems for higher-order integro-diferential equations, Applied Mathematics and Computation 118 (2001) 327–342.